Manuscript Details

Manuscript number	MTCOMM_2020_92
Title	Optimizing the antimicrobial performance of metallic glass composites through laser texturing
Article type	Full Length Article

Abstract

The influence of laser texturing on the physicochemical and bactericidal properties of Cu55Zr40Al5 Bulk Metallic Glass Composite (BMGC) to develop novel antimicrobial touch surfaces has been analysed. Laser ablation was employed to increase the average roughness of BMGC samples from 0.08 ± 0.02 μm to 3.07 ± 0.96 μm using a maximum laser fluence of 2.82 J/cm2. This results in the formation of CuO, CuO2, ZrO2, more prominent as the laser fluence was increased. The initial contact angle of the as-cast sample was increased from 85.81° to between 105.72° and 126.17° after texturing. The influence on the antimicrobial performance of all the samples was studied with Escherichia coli K12 modified to drive lux expression. Luminescence measurements indicated a reduction in bacterial growth as the laser fluence applied to the structured area was risen. This increase in bactericidal effect as laser fluence rose was corroborated with recovery tests, causing an increase in log reduction of E. coli K12 bacteria from 1.10 (for as-cast sample) to 2.16 (textured at 2.82 J/cm2) after 4h of contact. A length increase of E. coli cells from 2 μm up to 20 μm could be observed in SEM for cells deposited on the textured surfaces.

Keywords	Laser texturing; Bulk Metallic Glass Composite; Antimicrobial behaviour
Manuscript category	Metals and alloys
Corresponding Author	Sergio Gonzalez
Corresponding Author's Institution	Northumbria University
Order of Authors	Sergio Gonzalez
Suggested reviewers	Hamidreza Shahverdi, Aymen Tekaya, Reza Gholamipour

Submission Files Included in this PDF

File Name [File Type]

Cover letter.doc [Cover Letter]

Response to reviewers.docx [Response to Reviewers]

Highlights.docx [Highlights]

Paper text and Figures.docx [Manuscript File]

G_Abstract v2.tif [Figure]

F1.tif [Figure]

F2.tif [Figure]

F3.tif [Figure]

F4.tif [Figure]

Conflict of Interest.doc [Conflict of Interest]

Declaration-of-competing-interests.docx [e-Component]

To view all the submission files, including those not included in the PDF, click on the manuscript title on your EVISE Homepage, then click 'Download zip file'.

Research Data Related to this Submission

There are no linked research data sets for this submission. The following reason is given:
Data will be made available on request

Editor

Materials and design

20th December 2020

Dear Prof. Gibson,

Please find attached the manuscript entitled "Optimizing the antimicrobial performance of metallic glass composites through laser texturing", authored by Victor M. Villapún[a,*], Bokun Qu, Peter A. Lund, W. Wei, L.G. Dover, Jonathan R. Thompson, Janet O. Adesina, C. Hoerdemann, S. Cox, S. González which we would like you to consider for publication in *Materials@Design*.

This manuscript aims to study the influence of laser texturing on the physicochemical and bactericidal properties of $Cu_{55}Zr_{40}Al_5$ Bulk Metallic Glass Composite (BMGC) to develop novel antimicrobial touch surfaces. We have observed that an increase in laser fluence from 0.70 to 2.82 J/cm^2 leads to a linear rise in average roughness from 0.81 ± 0.22 μm to 3.07 ± 0.96 μm and formation of oxides on the sample surface, specifically CuO, Cu_2O and ZrO_2. This has led to physicochemical changes resulting in highly hydrophobic surfaces with contact angles between 105 to 126° compared with 86° for the non-ablated sample. Antimicrobial analysis based on recovery tests indicate that the antimicrobial properties when increasing the laser fluence from 0.70 to 2.82 J/cm^2, rises from a 1.10 to a 2.16 log reduction.

We have shown that combined use of recovery tests and microscopy studies and bioluminescence measurements has enabled a more complete assessment of the antimicrobial performance of these novel surface engineered surfaces. The present results reveal that laser texturing is a promising technique to enhance the antimicrobial properties of Cu-based BMGCs, which could be exploited to tackle nosocomial infections and antibiotic resistance.

From all the aforementioned reasons, we believe our study will have a high impact on the scientific community and therefore should be suitable for publication in *Materials@Design*.

Yours Sincerely,

Dr. Sergio González Sánchez

Department of Mechanical & Construction Engineering,
Wynne Jones Building,
Northumbria University,
Newcastle upon Tyne,
NE1 8ST, United Kingdom

Tel : + 44 (0) 191 349 5937
Email: sergio.sanchez@northumbria.ac.uk; sergiogs10@yahoo.es

Dear Editor and Reviewers,

Please find attached the manuscript entitled "Optimizing the antimicrobial performance of metallic glass composites through surface texturing", authored by Victor M. Villapún, Bokun Qu, Peter A. Lund, W. Wei, L.G. Dover, Jonathan R. Thompson, Janet O. Adesina, C. Hoerdemann, S. Cox, S. González, which we would like you to consider for publication in *Materials Today Communications*.

We appreciate the reviewers and Editors for their valuable comments and sound suggestions on our manuscript. We have carefully revised the manuscript according to the comments and suggestions. ***The revised parts are highlighted in red.*** The comments and the corresponding revisions are listed as follows:

Reviewers' comments:

Although this is a potentially interesting and well-prepared paper, the levels of impact and novelty are insufficient for publication in JMAD. However, submission to a different journal should be viable.

The Graphical Abstract contains too much material, some of which is insufficiently legible. A simpler, more effective GA is needed.

Thank you for your comment. The Graphical Abstract is now simpler and much more legible.

The original manuscript has been carefully revised according to the comments and suggestions. We look forward to hearing from you at your earliest convenience.

Yours Sincerely,

Dr. Sergio González Sánchez
Department of Mechanical & Construction Engineering,
Wynne Jones Building,
Northumbria University,
Newcastle upon Tyne,
NE1 8ST, United Kingdom
Tel : + 44 (0) 191 349 5937
Email: sergio.sanchez@northumbria.ac.uk;

Highlights:

- The influence of laser texturing a Metallic Glass Composite on the bactericidal properties has been analysed.
- Bioluminescence measurements indicated bacterial growth reduction on all laser textured surfaces from a 1.10 to a 2.16 log.
- Combined use of bioluminescence measurements, recovery tests and microscopy studies has enabled a more complete antimicrobial assessment.

Optimizing the antimicrobial performance of metallic glass composites through surface texturing

Victor M. Villapún[a,*], Bokun Qu.[a], Peter A. Lund[b] W. Wei[c], L.G. Dover[d], Jonathan R. Thompson[d], Janet O. Adesina[d], C. Hoerdemann[c], S. Cox[a], S. González[e,*]

[a]School of Chemical Engineering, University of Birmingham, Edgbaston B15 2TT, United Kingdom
[b]School of Biosciences, University of Birmingham, Edgbaston B15 2TT, United Kingdom
[c]Fraunhofer-Institut für Lasertechnik ILT
[d]Faculty of Health and Life Sciences, Northumbria University, Newcastle upon Tyne NE1 8ST, UK
[e]Faculty of Engineering and Environment, Northumbria University, Newcastle upon Tyne NE1 8ST, UK.

Corresponding author

Victor M. Villapún: v.m.villapun@bham.ac.uk

S. González: sergio.sanchez@northumbria.ac.uk

Abstract

In the present work, we analyse the influence of laser texturing on the physicochemical and bactericidal properties of $Cu_{55}Zr_{40}Al_5$ Bulk Metallic Glass Composite (BMGC) to develop novel antimicrobial touch surfaces. Laser ablation was employed to increase the average roughness of BMGC samples from 0.08 ± 0.02 µm to 3.07 ± 0.96 µm using a maximum laser fluence of 2.82 J/cm^2. This treatment also influenced surface chemistry with formation of CuO, CuO_2, ZrO_2, more prominent as the laser fluence was increased. Alongside chemical and topographic changes, the initial contact angle of the as-cast sample was increased from 85.81° to angles between 105.72° and 126.17° after texturing. The influence of these modifications on the antimicrobial performance of all rapidly solidified alloys was studied with *Escherichia coli K12* modified to drive lux expression. Luminescence measurements indicated a reduction in bacterial growth as the laser fluence applied to the structured area was risen. This increase in bactericidal effect as laser fluence rose was corroborated with recovery tests, causing an increase in log reduction of *E. coli K12* bacteria from 1.10 (for as-cast sample) to 2.16 (textured at 2.82 J/cm^2) after 4h of contact. Variations on the bacterial morphology were observed with SEM imaging, specifically, a length increase of *E. coli* cells from 2 µm up to 20 µm could be observed on cells deposited on the textured surfaces. Deposited bacteria on laser treated samples revealed loss of

membrane integrity, which along the morphological changes suggest both external and DNA damage in all ablated samples. These findings reveal the possibility of tailoring the antimicrobial behaviour of BMGCs through the use of laser texturing, which could be used as novel touch surfaces to tackle nosocomial infections along antibiotic resistance.

1. Introduction

Nosocomial infections or healthcare acquired infections (HAI) are those that patients acquire during a healthcare treatment. Statistics have shown that at least 300 thousand patients in England suffer HAI, while in the US 1.7 million people experience a HAI every year [1-3]. The impact of nosocomial infections is further aggravated by the emergence of antibiotic resistant bacteria, some of which can tolerate last resort antibiotics. Recent reports highlight the socioeconomic impact of antibiotic resistance with global costs predicted to reach 100 trillion $ and 10 million lives annually by 2050 [4, 5]. Selection of different antibiotics has been the main pathway chosen to tackle resistance, nonetheless, the speed in the discovery of novel antibiotics has been greatly reduced, driving an urgent need for other antimicrobial agents. An alternative approach to traditional antibiotics is to use antimicrobial materials such as copper that due to its promising efficacy and multiple mechanisms of action has started to be implemented in healthcare facilities as touch surfaces [6-8]. However, the low wear resistance of copper endangers its long term applicability, which could be addressed by developing Metallic Glass Composites (MGCs) with optimum size and volume fraction of amorphous phase [9].

Fully amorphous alloys or Metallic Glasses (MGs) do not exhibit the regular structure of crystalline materials, conferring superior mechanical and tribological properties [10, 11]. Nevertheless, the inhomogeneous plastic deformation caused by shear banding in MGs makes them brittle while a lack of grain boundaries limits copper ion diffusion into bacteria and thus its antimicrobial activity. In this regard, the introduction of crystalline phases onto an amorphous matrix, Bulk Metallic Glass Composites (BMGCs), has made it possible to limit shear band localization. Moreover, optimizing the volume fraction of the crystalline phase enables unification of the high bactericidal effect of copper with the superior mechanical behaviour of BMGs [12, 13]. More recently surface modification in the form of laser texturing has demonstrated its

capability to reduce BMGs brittleness. As shown by Wu et al. [14], the high temperatures achieved during laser and surface interaction are able to redistribute residual stresses, increase free volume and, in some cases, produce partial crystallization of the material, altering the inhomogeneous shear banding inherent to MGs. Laser texturing also enables modification of surface topography, chemistry and, as such, the surface wettability all of which have been shown to influence bacterial attachment [15-17]. Nevertheless, modification of BMGs and BMGCs through laser texturing is still an emerging field where both experimental [18] and computational modelling studies [19] are underway.

The versatility of laser texturing to produce complex geometries is of great interest to optimize touch surfaces. Nevertheless, the relationship between surface finish and bacterial attachment is still controversial and mixed observations can be found in the literature. Average roughness (R_a) in the nano to microscale (0.04 to 3 μm) generally leads to increased bacterial adhesion for rougher surfaces [20, 21]. However, other authors have observed that coarser features, up to 8 μm, can reduce the proliferation of some bacterial species [22, 23]. Although this relationship is still not completely understood, changes in surface finish can modify the wettability of the material. Kubiak et al. [24] had demonstrated that roughness modification can be used to change the complete wetting mode typical of hydrophilic (contact angle <90°) surfaces into a double wetting mode common in hydrophobic (contact angle >90°) surfaces. There is still controversy about the relationship between hydrophobicity and bacterial adhesion since it depends on various parameters, including the material chemistry. Nevertheless, hydrophobic materials are generally considered less prone to bacterial adhesion than hydrophilic surfaces [25, 26]. At the same time, previous studies have demonstrated the possibility of tuning the antimicrobial properties of BMGCs through crystalline phase control [9, 12] and oxidation [27]. The ability of laser texturing to affect all these physicochemical properties and, thus, bacterial colonization makes it a technology of interest in HAI prevention.

In this paper, the role of laser fluence on the physicochemical and antimicrobial properties of a Cu-based BMGCs has been studied. The number of studies about laser texturing in metallic glasses is relatively scarce and, as far as the authors are aware, its influence on the antimicrobial behaviour of rapidly solidified composites has not

been studied before. This knowledge will be useful for the development of antimicrobial surfaces for hospitals and other healthcare settings.

2. Experimental section

2.1. Laser texturing

Alloy ingots of nominal composition $Cu_{55}Zr_{40}Al_5$ at. % were prepared from elements with purity higher than 99.9 at. %. The master alloy was re-melted three times in a Zr-gettered high purity argon atmosphere to improve chemical homogeneity. Rod samples of 2 mm were obtained from the master alloy by copper mould casting in an inert gas atmosphere with a cooling system set at 10°C. The resulting rod was sliced and each surface ground through a series of grit papers (P240, P600, P1200 and P4000). Texturing was performed through laser ablation (PHAROS, Light Conversion, Vilnius, Lithuania) on the polished surfaces with a repetition frequency of 200 kHz, wavelength of 1028 nm, pulse duration of 200 fs and a spot diameter of 33 μm. To texture the Cu-based bulk metallic glass composites, three different laser fluence conditions were used (Table 1). For simplicity, samples have been coded as T1, T2 and T3 for increasingly laser fluence values.

Table 1 Summary of the laser processing conditions used to texture the Cu-based BMGC.

Sample	Laser fluence (J/cm^2)	Scanning speed (mm/s)	Scanning interval (μm)
Type 1	0.7	20	10
Type 2	1.39	20	10
Type 3	2.82	20	10

The obtained microstructure was studied by X-ray diffraction (XRD) using a Siemens D5000 diffractometer with Cu Kα radiation (λ = 1.54184 Å) at 40 kV and 40 mA, with a scanning speed of 0.01°/s in the 2θ range 35° to 80°. Roughness of all prepared samples was analyzed using a non-contact profilometer (InfiniteFocus G5, Alicona UK, Seven oaks, United Kingdom) and results were obtained by averaging 20 independent measurements.

Surface finish and compositional analysis was performed using a Tescan Mira 3, Scanning Electron Microscope (SEM) with 20 kV of acceleration voltage, equipped with an Oxford Instruments X-Max 150 Energy Dispersive X-ray (EDX) detector. Contact angle measurements were carried out using the sessile drop technique (Krüss drop size DSA30 analyser). To ensure that the contact angle measured came from the natural interaction between liquid and surface, a two-step method was used. Firstly, 1 µL of deionised water was dispersed on air at a rate of 30 µL/min. The droplet was moved onto the surface of interest and then 1 µL more of liquid was dispersed. Contact angle measurements were immediately observed to prevent droplet shape change due to evaporation and results averaged from ten sessile drop tests.

2.2. Fluorescence and antimicrobial tests

For all microbiology tests, *Escherichia coli K12* MG1655 transformed with a plasmid carrying a kanamycin resistance marker and a constitutive promoter from the *acpP* gene driving expression of a luciferase operon was used [28]. Mueller Hinton (MH) media was prepared as per standard methods with 50 µg/ml Kanamycin. Bacteria were cultivated overnight in an orbital incubator (37°C, 200 rpm), diluted to an OD_{600} of 0.01 and left to grow until an OD_{600} of 0.3 was achieved. BMGCs and control sample (stainless steel) were immersed in 100% ethanol and sonicated for 5 min in an ultrasound bath to ensure a clear and disinfected surface. Sterilised samples were left to dry in a petri dish before further testing. 2 µL of inoculum were deposited on each sample placed inside a 48 well plate and 1 mL of sterile PBS added to adjacent wells to prevent inoculum drying. The well plate was then sealed with film and bioluminescence observed using a TECAN Spark plate reader (Tecan Trading AG, Switzerland) in luminescence mode, Counts/s, every 5 min during 2 h. Results were the average of three samples with mean counts and standard deviation reported.

Antimicrobial tests were performed with the previously mentioned *Escherichia coli* strain. A quantity of 2 µL of these cultures was dispensed directly onto the BMGC and control (stainless steel) surfaces and incubated at room temperature in sealed petri dishes containing sterile tissue wetted with 1 mL of PBS. After the designated exposure time, the samples were placed into an Eppendorf filled with 99 µL of Tween 20, 0.148 g/L (2 × CMC), and sonicated for 5 min. Finally, the recovered bacterial suspension was subjected to serial decimal dilution and spread onto MH agar plates

modified with 50 µg/ml of Kanamycin. Resulting colonies were counted after 16 h of incubation time at 37°C. All tests were performed three times, with mean counts and standard deviation reported.

To analyse the influence of texturing on the morphology of *E. coli*, one sample per condition was observed by SEM. After cultivation, each sample was washed gently three times with 10 mM PBS, fixed with 2.5% glutaraldehyde in cacodylate buffer for 1 h, dehydrated with a series of ethanol and deionized water dilutions (10 minutes in 20, 30, 40, 50, 60, 70, 90, 95 and 100 %), treated with hexamethyldisilzane and dried overnight. Samples were gold coated and SEM images taken at 10kV acceleration voltage with an EVO M10 system (Zeiss International, Birmingham).

3. Results and discussion

3.1. Microstructure and surface texturing

Figure 1 shows the SEM images of the stainless-steel control sample and textured $Cu_{55}Zr_{40}Al_5$ at. % substrates along with the corresponding optical profilometry images and average roughness values (R_a). In order to assess differences in antimicrobial performance between textured and base materials, a control sample, stainless steel (surface roughness in as-received conditions: casted and rolled), 0.14 ± 0.02 µm, and a metallic glass composite (BMGC), 0.08 ± 0.02 µm, were used. The surface finish of the treated BMGCs becomes coarser with increasing laser fluence, alongside differences in topographic features. Specifically, the surface obtained with a laser fluence of 0.70 J/cm^2 shows a repetitive pattern based on long lines of small islands of re-melted alloy with an average roughness of 0.81 ± 0.22 µm. These microgrooves and protrusions are formed after laser texturing as a result of the applied laser fluence distribution and the subsequent vaporization of the processed material. However, the relatively high laser power used has led to a non-uniform wrinkled surface similar to that already reported in the literature [29, 30]. An increase of laser fluence to 1.39 J/cm^2 caused a rise in average roughness, 1.70 ± 0.48 µm, but the obtained texture is more irregular with broader (up to 60 µm) grooves and triangle shaped islands. This increase in groove width is maximum for the T3 sample (2.82 J/cm^2) and about 100 µm, however, tall columns of up to 20 µm between grooves can be seen. This results in a maximum average roughness of 3.07 ± 0.96 µm, which coupled with the fact that

the first Cone Like Protrusions (CLP) structures begin to form at this point indicate an increased ablation rate due to the modifications of the laser fluence [31]. The textured surface of the samples is highly dependent on the selected laser fluence used (T1: 0.70, T2: 1.39 and T3: 2.82 J/cm^2) and, interestingly, there is a linear correlation between this processing parameter and average roughness (R^2 = 99.41%).

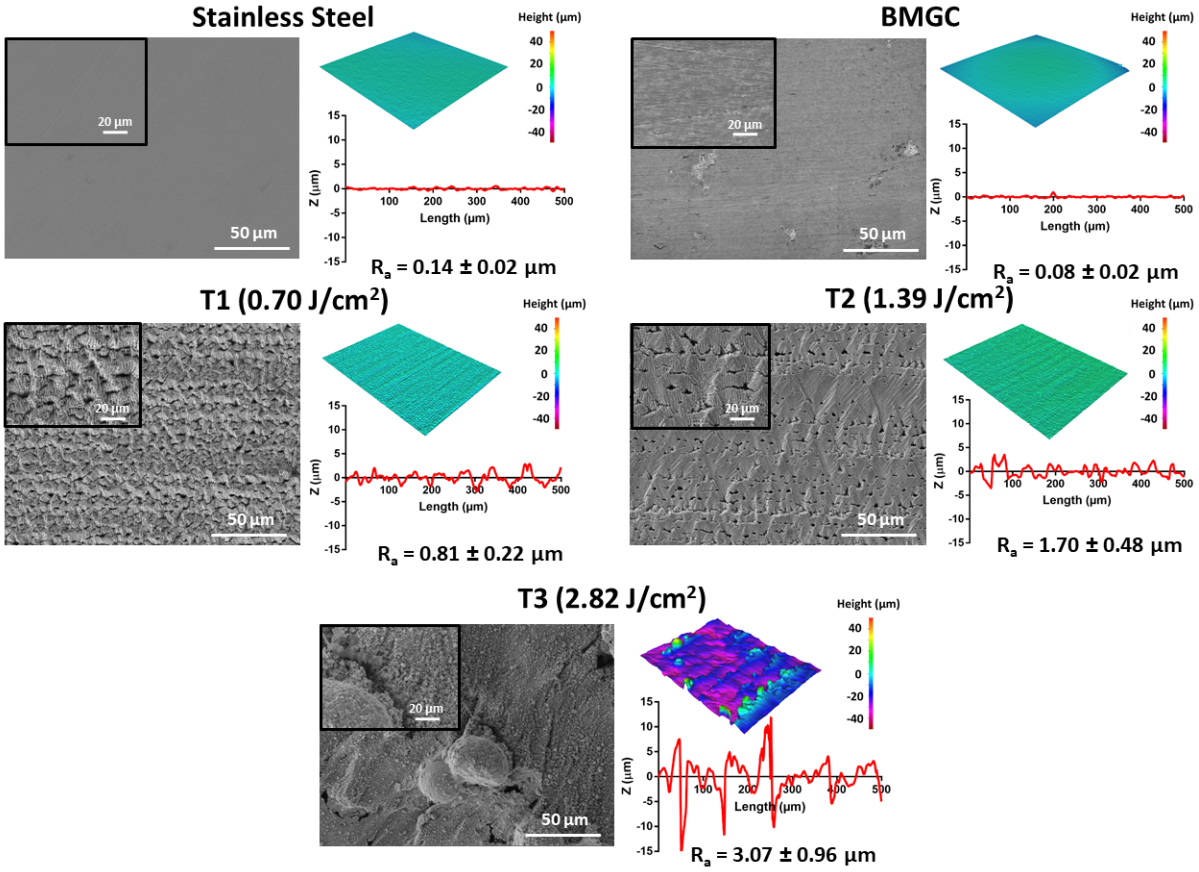

Figure 1 Surface topographies for stainless steel, for as-cast $Cu_{55}Zr_{40}Al_5$ at. % BMGC and after texturing at T1, T2 and T3 laser conditions, SEM and profilometer scans alongside average roughness, R_a, and a roughness profile.

The use of laser ablation has effectively modified the surface of all BMGCs into repeatable structures. Figure 1 shows the presence of a fine structure on top of the patterning, especially relevant on the T3 sample. In order to explain this hierarchical structure, consisting of a surface pattern and smaller surface features, the role of the thermodynamic critical temperature (T_{tc}) has to be taken into consideration. This parameter can be defined as the temperature from which the vapour growth rate increases exponentially during laser ablation, and it has been suggested that as the processing temperature approaches this value, the main phenomenon dominating the surface texture varies. For picosecond laser sources with more than 12 ps and for lower T_{tc} values, the alloy goes through melting and then vaporization, but as it passes T_{tc}, sublimation takes place, resulting in explosive boiling. Lower energy fluences and short pulse durations commonly led to vaporization for Vitreloy 1 BMG, as shown by Williams et al. [32]. In the present case, a femtosecond (200 fs) laser has been used with a relatively low fluence level, suggesting that during texturing of the T1, T2 and T3 samples no melting phase dominated the formation of the final surfaces. This along the SEM images (Figure 1) indicate that the temperature reached by the laser treatment is not near the T_{tc}, ensuring that no explosive boiling has taken place. Thus, the secondary roughness feature will be caused by the photon phonon interaction of the treated material and the applied laser fluence. Ultra-short pulsed laser ablation promotes the development of self-organizing microstructures. Depending on the fluence, the accumulated energy and the number of laser passes, laser induced periodic surface structures (LIPSS) and cone-like protrusions (CLPs) are created on the surface. It must be said that for nanosecond pulsed laser experiments instead of ultra-short pulsed laser tests, the secondary roughness feature has been attributed to the re-solidification of vaporized alloy, observed in other BMGs by Huang et al. [30]. Besides the topographical changes described, the samples were processed in air and therefore due to the high temperatures achieved upon texturing they are prone to oxidation. To investigate the nature of any potential surface change, XRD scans before and after texturing were performed (Figure 2).

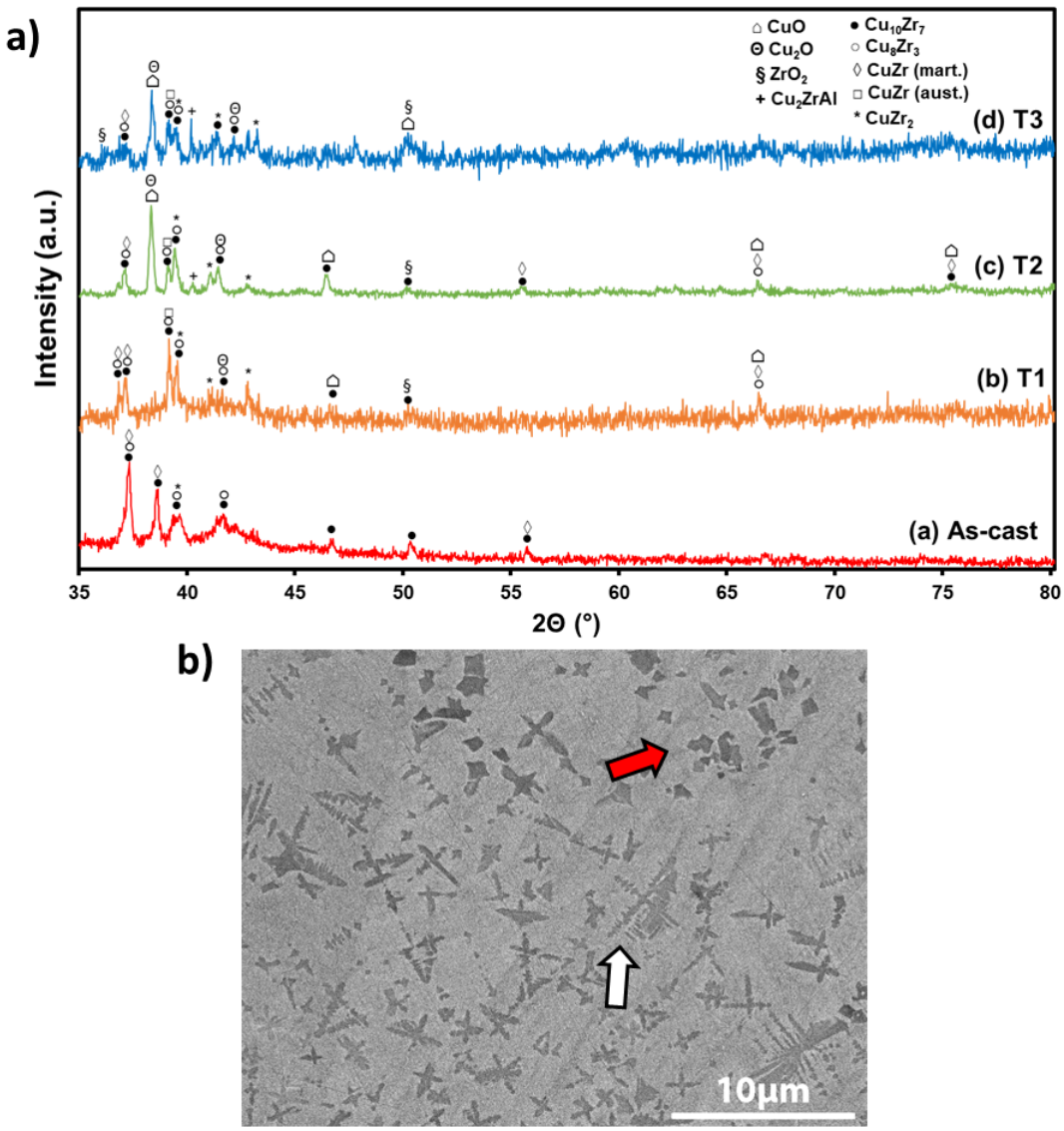

Figure 2 (a) XRD scans for the 2 mm diameter as-cast $Cu_{55}Zr_{40}Al_5$ BMGC before and after texturing at T1, T2 and T3 conditions (b) representative backscattered SEM image of the as-cast sample.

Figure 2a shows the XRD scans of the as-cast and textured alloys. For the as-cast sample, a relatively low amorphous hump from 40-45° can be noticed while the presence of multiple high intensity peaks suggest the existence of crystalline phases embedded in the amorphous matrix. This agrees with the backscattered SEM image (Figure 2b) obtained from the middle radius of the as-cast $Cu_{55}Zr_{40}Al_5$ BMGC. For all samples, the following phases have been detected: orthorhombic $Cu_{10}Zr_7$ (a = 0.9347 nm, b = 0.9347 nm, c = 1.2675 nm), orthorhombic Cu_8Zr_3 (a = 0.78686 nm, b = 0.81467 nm, c = 0.9977 nm), austenite B2 CuZr (a = 3.2562 nm, b = 3.2562 nm, c = 3.2562 nm), monoclinic martensite B19´ CuZr (a = 0.3237 nm, b = 0.4138 nm, c = 0.5449 nm)

and tetragonal $CuZr_2$ (a = 0.3220 nm, b = 0.3220 nm, c = 1.1183 nm). The microstructure of the base alloy consists of cubic (red arrow) and dendritic (white arrow) particles up to 10 μm in size embedded in a featureless matrix. According to EDX analysis, the composition of the cubic particle is $Cu_{36.2}Zr_{51.0}Al_{12.8}$ at. % and therefore could be attributed to $CuZr_2$, while the dendritic phases (white arrow) have similar concentration of Cu and Zr (i.e., $Cu_{46.3}Zr_{41.1}Al_{4.7}$) and thus could correspond to CuZr [9].

Subsequent laser texturing of all samples was conducted in air and therefore surface heating has led to partial oxidation. This is revealed by the presence of new XRD peaks corresponding to monoclinic CuO (a = 0.4653 nm, b = 0.3410 nm, c = 0.5108 nm), cubic Cu_2O (a = 0.4252 nm, b = 0.4252 nm, c = 0.4252 nm) and tetragonal ZrO_2 (a = 0.5070 nm, b = 0.5070 nm, c = 0.5160 nm), similar to those reported by Fornell et al. [33]. The composition of the matrix far from the crystalline phases (i.e., $Cu_{54.9}Zr_{40.2}Al_{4.9}$ at. %) is similar to the nominal composition. A significant decrease in the intensity of the amorphous hump after texturing at T1 conditions suggests the surface temperature is high enough to change the microstructure. This behaviour is even more noticeable when the laser fluence increases to 1.39 and 2.82 J/cm^2 (T2 and T3, respectively) as can be seen from the lack of amorphous hump in the XRD scans. This indicates that the amorphous phase has crystallized, which is consistent with the detection of an additional peak at about 41° associated to cubic Cu_2ZrAl (a = 0.6190 nm, b = 0.6190 nm, c = 0.6190 nm) for the T2 condition and whose intensity increases for T3. Laser texturing at higher fluences also increases the volume fraction of oxides. The intensity of the oxide peaks are relatively low for the sample patterned at 0.70 J/cm^2 (T1), but they increase significantly for higher laser fluences. In fact, for T2 and T3 conditions, a peak at about 39° is detected, which can be associated with CuO and Cu_2O, suggesting that the volume fraction of oxides has increased. The formation of oxides after texturing is supported by EDX results (Table 2) due to the detection of high concentrations of oxygen. EDX measurements indicate a reduction in Zr as the laser fluence rises with little changes in copper content, which along the previously commented XRD (Figure 2a) suggest larger amounts of copper oxides. The concentration of oxygen increases from 24.5 ± 2.1 at. % for T1 to 41.3 ± 6.0 at. % and 36.4 ± 1.0 at. % for T2 and T3, respectively. For T2 the values are slightly smaller but

about within the error range of T3, thus suggesting that beyond certain laser fluence the oxidation stabilizes. However, the formed oxide layer is brittle in nature and tends to come off when a thick layer develops, which may play an important role in this sudden reduction [27]. The change in crystalline phases including both copper and zirconia oxides coupled with our previous analysis of Cu-based BMGCs oxidation [27] indicates formation of a multi-layered oxide configuration. Such structure is commonly observed in heat treated BMGCs and explained by differences in formation enthalpies ($\Delta H_f(ZrO_2)$=-1100.8kJ/mol, $\Delta H_f(CuO_2)$=-167.4kJ/mol and $\Delta H_f(CuO)$=-155.2kJ/mol) [33, 34].

Table 2 Compositional analysis (at. %) of the Cu-based BMGCs before (as-cast) and after (T1, T2 and T3) laser texturing

	O	Al	Cu	Zr
As-cast	-	4.9 ± 0.2	54.9 ± 0.5	40.2 ± 0.4
T1	24.5 ± 2.1	3.2 ± 0.2	50.5 ± 2.3	21.8 ± 1.3
T2	41.3 ± 6.0	2.0 ± 0.3	44.2 ± 6.1	12.4 ± 0.7
T3	36.4 ± 1.0	2.7 ± 0.1	42.7 ± 1.5	18.3 ± 0.4

3.2. Wettability

Bacterial adhesion is a fundamental aspect in antimicrobial surface development and therefore wettability is a relevant property to optimize. For this reason, the wettability of all samples was estimated using the sessile drop technique with deionized water to measure static contact angle (Figure 3). The contact angle of the as-cast sample and stainless steel control are similar (85.81 ± 4.18° and 80.67 ± 3.35, respectively), but smaller than those obtained for the textured surfaces: 126.17 ± 6.88° (T1), 105.72 ± 6.14° (T2) and 118.11 ± 5.60° (T3). This change from hydrophilic to hydrophobic contact angle is common in laser texturing, although the obtained values are slightly lower than those exhibited by textured BMGs [29].

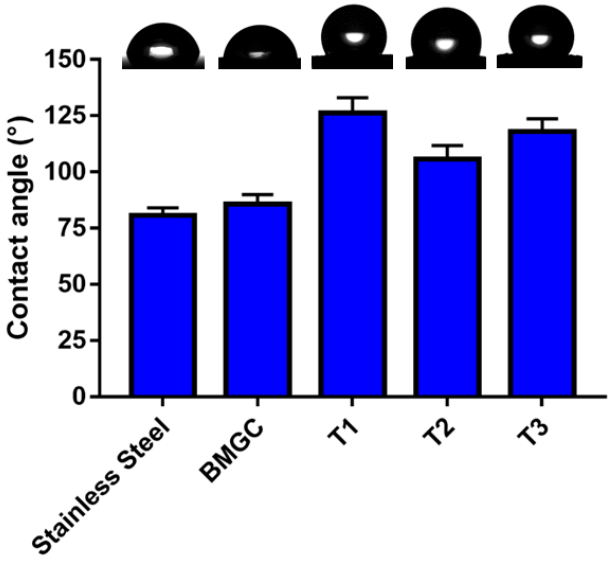

Figure 3 Water contact angle obtained for stainless steel, as-cast and patterned Cu-based BMGC including details of the measured droplets.

Table 3 Water contact angle measured for stainless steel, as-cast and patterned Cu-based BMGC.

	Contact angle (°)
Stainless Steel	80.67 ± 3.35
BMGC	85.81 ± 4.18
T1	126.17 ± 6.88
T2	105.72 ± 6.14
T3	118.11 ± 5.6

The processing of the BMGCs through laser texturing has led to highly hydrophobic surfaces, however, in contrast to the average roughness, this modification is not linearly related to the increase in laser fluence. Patterned surfaces generally display hydrophobic properties [35-37], however, the ability of a liquid to wet a surface is a complex process dependent on numerous parameters (i.e. surface chemistry, interfacial energy, topographic features) [38]. Variations on roughness and as such, wetting modes, can be one of the driving mechanisms behind this change to hydrophobic surfaces. Engineered materials displaying low roughness typically lead to homogeneous surface wetting as described in Wenzel's model [39]. In contrast, a rise in roughness will provide spaces where air can become entrapped, leading to a double interaction at surface-liquid and liquid-air interfaces common on hydrophobic surfaces and explained by Cassie-Baxter's theory [40]. This change from hydrophilic

to hydrophobic contact angle due to surface modification alone is not unusual and can be found in other engineering surfaces [24].

Besides topographical changes, chemistry also plays a fundamental role in wettability. Romano et al. [41] analysis of textured stainless steel surfaces had demonstrated that variations in contact angle can be explained by chemical changes on the surface. In their work, they showed that hydrocarbon molecules from air can attach to the roughened surface structures, forming an organic layer that modifies the hydrophilic surface onto hydrophobic or even superhydrophobic. At the same time, the stability of contact angle in Cu-based textured surfaces has been shown to be highly dependent on the exposure time to ambient conditions, leading to increases of about 100-120 degrees after 20 days of processing (i.e. 20 degrees to 140 degrees) [42, 43]. These authors stated this change could be attributed to the partial deoxidation of CuO into Cu_2O through the following reaction:

$$2CuO \leftrightarrow Cu_2O + ½\ O_2$$

As previously observed by Chang et al. [44], Cu_2O exhibits hydrophobic properties while CuO is highly hydrophilic. The heterogeneous structure caused by the deoxidation of the surface will consist of regions with different atomic percentages of CuO and Cu_2O. For the studied samples, an increase in oxidation and roughness takes place simultaneously, which could lead to the hydrophobicity detected in Figure 3. As for the lower contact angle displayed by the T2 sample, Kubiak et al. [24] reported that high contact angles would be found for small and high roughness with a minimum in the intermediate roughness values. This minimum can be found for average roughness around 1 μm, depending on the material surface [24]. For the textured samples, the T2 sample roughness, 1.70 ± 0.48 μm, will be near this value, while the T1 and T3 samples would be on the sides of the contact angle vs roughness curve, explaining the changes in wettability found in Figure 3.

3.3. Antimicrobial behaviour

The antimicrobial properties of all samples were analysed through several studies, namely bioluminescence measurements, assessment of recovered colony forming units (CFUs) and SEM imaging (Figure 4). To understand the biocidal performance

during the initial stages of contact, bioluminescence of the modified *E. coli K12* strain was measured for up to two hours, 7200 seconds, (Figure 4a).

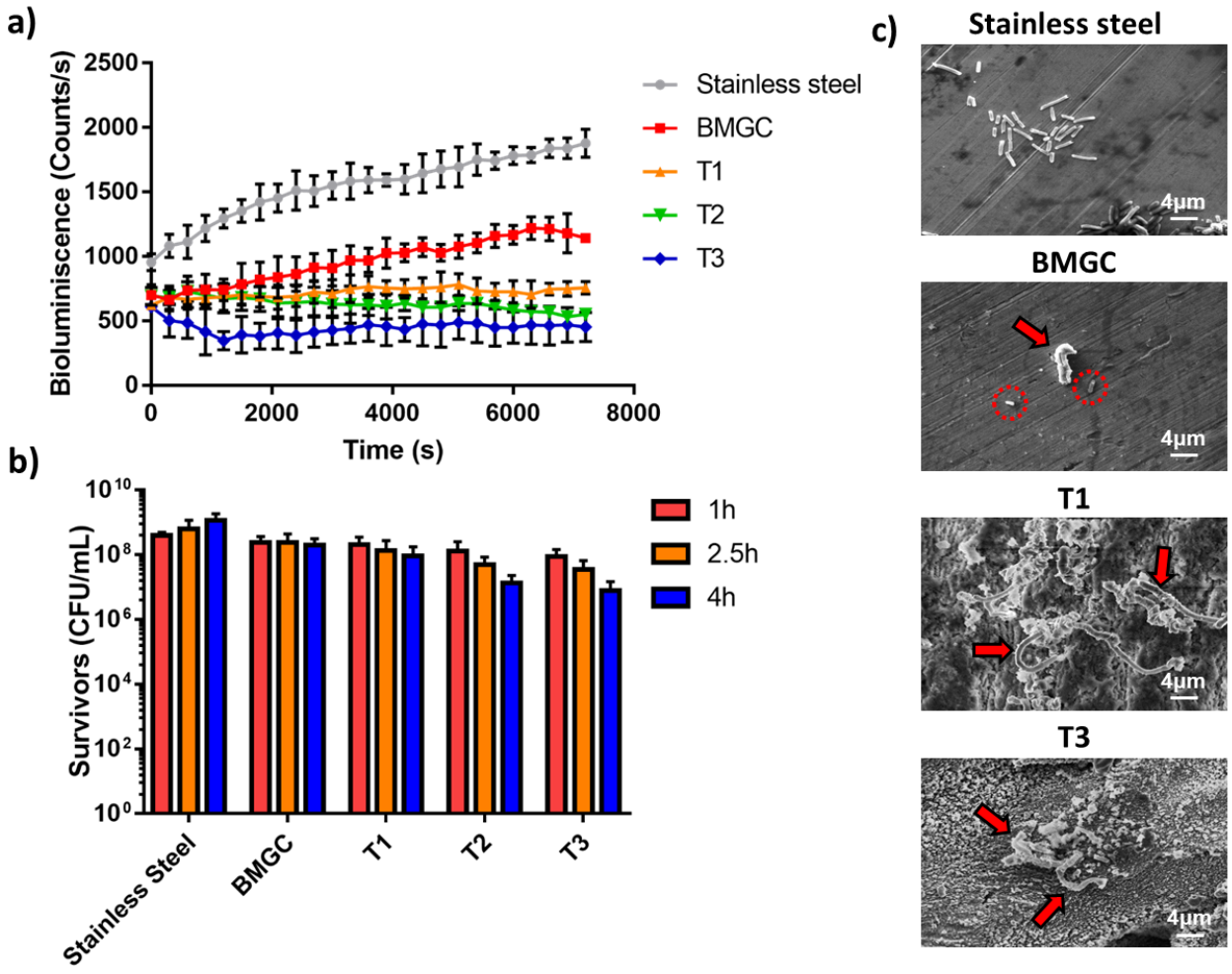

Figure 4 (a) Bioluminescence measurements for the analysed samples, (b) *E. coli* colony forming units recovered after 1, 2.5 and 4 h of contact and (c) SEM images of deposited bacteria after 4 h of contact.

The luminescence displayed by bacteria deposited on stainless steel shows a steady increase following inoculation. As bioluminescence is emitted naturally by active cells and variations in luminosity depend on changes in bacterial population [45], this increase indicates that bacteria are still growing over the contact time. A similar increase is observed on the as-cast BMGC, however, the slope is less prominent than for stainless steel and starts to decay after two hours. Stainless steel lacks any bactericidal effect and, as such, was used as reference material. This therefore suggests that the as fabricated BMGC has some early inhibitory and antimicrobial behaviour, which is consistent with previous observations [9]. In contrast, the laser ablated BMGCs display more flat curves with average bioluminescence values of

719.92 ± 78.04 Counts/s (T1), 631.65 ± 80.35 Counts/s (T2) and 449.72 ± 117.65 Counts/s (T3). This suggests that an increase of the laser texture fluence from 0.70 J/cm^2 to 2.82 J/cm^2 enhances the antimicrobial performance.

These bioluminescence assays were complemented with bacteria recovery and quantification after 1, 2.5 and 4 hours of contact between sample and *E. coli* cells (Figure 4b). The number of Colony Forming Units per millilitre (CFU/mL) recovered on the control steel surface increases during the timeframes analysed, from 3.93*10^8 ± 1.04*10^8 CFU/mL to 1.17*10^9 ± 7.08*10^9 CFU/mL after 1 h and 4 h of contact respectively, corroborating the trend observed on the bioluminescence curves. The number of CFU/mL obtained for the as-cast BMGC sample do not vary during 2.5 hours of contact (~2.41*10^8 CFU/mL), but shows a slight reduction after 4 hours (2.03*10^8 ± 1.12*10^8 CFU/mL), consistent with the limited contact killing displayed in the bioluminescence assays (Figure 4a) and previous observations [9, 12]. In contrast, laser texturing has caused varying degrees of reduction in CFU/mL as the contact time increases. This is lower on the T1 sample (from 2.05*10^8 ± 1.44*10^8 CFU/mL to 9.36*10^7 ± 8.26*10^7 CFU/mL for 1 h and 4 h respectively), increasing for the T2 (1.33*10^8 ± 1.20*10^8 CFU/mL to 1.34*10^7 ± 9.76*10^6 CFU/mL for 1 h and 4 h respectively) and T3 (8.82*10^7 ± 5.68*10^7 CFU/mL to 8.04*10^6 ± 6.79*10^6 CFU/mL for 1 h and 4 h respectively) samples. The decrease in colony forming units, can be translated into a log reduction of 1.10 (T1), 1.94 (T2) and 2.16 (T3), which further supports the hypothesis that laser texturing has enhanced the bactericidal properties of the Cu-based BMGC.

Antimicrobial analysis of hard surfaces can be performed through a large range of tests, although there is a prevalence in using the JIS Z2801:2010 standard or the US EPA protocol [46, 47]. These tests involve relatively tedious inoculation and recovery to quantify the number of CFU/mL surviving contact between antimicrobial surface and bacterial strain. More recently, Rosenberg et al. [45] proposed the use of bioluminescence as a cost effective tool to speed up bactericidal quantification. Here a modified bioluminescence assay was prepared and compared with common recovery and quantification techniques. These analyses revealed the ability of bioluminescence assays to facilitate early quantification of antimicrobial properties of Cu-based BMGC, as seen by the lower slope of the as-cast sample and the reduction

in bioluminescence for the textured surfaces (Figure 4a). The reduction observed in standard recovery tests was similar, suggesting the applicability of bioluminescence in the antimicrobial field.

To investigate the effect of contact killing on the morphology of the deposited *E. coli* strain, SEM images were taken after 4 h of inoculation (Figure 4c). Cells deposited on the control surface are thin rods around 2 μm in length, typical of healthy *E. coli* bacteria. However, bacterial cells deposited on the as-cast Cu-based BMGC are shorter (dashed circles) and exhibit punctual aggregations (red arrow). These morphological changes are more prominent for the bacteria deposited on the T1 and T3 samples, displaying longer rods (up to 20 μm) with thicker and fuzzier membranes. Both features suggest that the deposited *E. coli* has suffered external and internal damage commonly mentioned in the literature as effects of copper dosage [48].

Both bioluminescence and recovery tests (Figures 4a and 4b) clearly show that laser texturing of a Cu-based BMGC has increased their antimicrobial behaviour. The bactericidal effect displayed can be influenced by the modification of roughness, wettability and chemical composition derived from the rise in laser fluence. These modifications have transformed the initially hydrophilic surfaces into hydrophobic, which are generally accepted as less prone to bacterial adhesion [25, 26], limiting the ability of bacteria to growth on the surface of the treated materials. In addition, the availability of copper ions will be increased by the presence of copper rich oxides as the concentration of copper is similar (for CuO) or higher (Cu_2O) than for the nominal composition ($Cu_{55}Zr_{40}Al_5$ at. %) of the BMGC. This effect will be further enhanced by the appearance of Cu_2O as the sample partially deoxidized [44], which has shown higher bactericidal behaviour than its CuO counterpart [49]. As the laser fluence was increased, the aforementioned physicochemical changes were exacerbated, leading to the reduction in luminescence and CFU/mL seen in Figure 4.

4. Conclusions

In this manuscript, the influence of laser ablation fluence on the surface finish, wettability and antimicrobial properties of $Cu_{55}Zr_{40}Al_5$ at. % bulk metallic glass

composites have been analysed. The following conclusions can be drawn for the present study:

- An increase in laser fluence from 0.70 to 2.82 J/cm^2 leds to a linear rise in average roughness from 0.81 ± 0.22 μm to 3.07 ± 0.96 μm, in a process dominated by vaporization of the base alloy.
- The rise in laser fluence caused the formation of oxides on the sample surface, specifically CuO, Cu_2O and ZrO_2.
- These physicochemical changes led to highly hydrophobic surfaces with contact angles between 105 to 126° compared with 86° for the non-ablated sample.
- Bioluminescence measurements indicated a population increase of *E. coli* on the stainless steel control, limited inhibition on the as-cast BMGCs and bacterial growth reduction on all laser textured surfaces.
- Bacterial recovery tests revealed that laser texturing was able to increase the antimicrobial properties of the base alloy, rising from a 1.10 to a 2.16 log reduction as the laser fluence increased from 0.70 to 2.82 J/cm^2, further supporting the bioluminescence tests.

Combined use of bioluminescence measurements, recovery tests and microscopy studies has enabled a more complete assessment of the antimicrobial performance of these novel surface engineered surfaces. The present results reveal that laser texturing is a promising technique to enhance the antimicrobial properties of Cu-based BMGCs, which could be exploited to tackle nosocomial infections and antibiotic resistance.

Acknowledgements

The authors acknowledge research support from Northumbria University and the University of Birmingham.

References

[1] R.M. Klevens, J.R. Edwards, C.L. Richards, Estimating health care-associated infections and deaths in U.S. hospitals, Public Health Rep. 122(2) (2002) 160–166

[2] M. Haque, M. Sartelli, J. McKimm, M.A. Bakar, Health care-associated infections–an overview, Infec. Drug Resist. 11 (2018) 2321.
[3] N.I.o.H.a.C.E. (NICE), Infection: Prevention and Control of Healthcare Associated Infections in Primary and Community Care, NICE, 2014.
[4] J. O'Neill, S. Davies, J. Rex, L.J. White, R. Murray, Review on antimicrobial resistance, tackling drug-resistant infections globally: final report and recommendations, Wellcome Trust and UK Government, London, 2016.
[5] R. Smith, J. Coast, The true cost of antimicrobial resistance, Bmj 316 (2013) f1493.
[6] C.E. Santo, E.W. Lam, C.G. Elowsky, D. Quaranta, D.W. Domaille, C.J. Chang, G. Grass, Bacterial killing by dry metallic copper surfaces, Appl. Environ. Microbiol. 77 (2011) 794–802.
[7] S.L. Warnes, C.W. Keevil, Inactivation of norovirus on dry copper alloy surfaces, Plos One 8 (2013) 1–8.
[8] T. Mori, T. Kikuchi, M. Sakurai, J. Kato, Y. Koda, R. Abe, C. Sumiya, R. Yamazaki, K. Sugita, N. Hasegawa, S. Okamoto, Bacteriocidal effects of introducing copper products on highly touched areas in hematology ward, Rinsho Ketsueki 60(1) (2019) 3-6.
[9] V.M. Villapún, F. Esat, S. Bull, L.G. Dover, S. Gonzalez, Tuning the mechanical and antimicrobial performance of a Cu-based metallic glass composite through cooling rate control and annealing, Materials 10(5) (2017) 506.
[10] J. Qiao, H. Jia, P.K. Liaw, Metallic glass matrix composites, Mater. Sci. Eng. R. 100 (2016) 1–69.
[11] T. Gloriant, Microhardness and abrasive wear resistance of metallic glasses and nanostructured composite materials, J. Non-Cryst. Solids 316 (2003) 96–103.
[12] V.M. Villapún, H. Zhang, C. Howden, L.C. Chow, F. Esat, P. Pérez, J. Sort, S. Bull, J. Stach, S. González, Antimicrobial and wear performance of Cu-Zr-Al metallic glass composites, Mater. Design 115 (2017) 93-102.
[13] V.M. Villapún, Rapidly solidified metallic glass alloys for antibacterial touching surfaces, Mechanical Engineering, Northumbria University, Newcastle upon Tyne, 2018.
[14] G. Wu, R. Li, Z. Liu, B. Chen, Y. Li, Y. Cai, T. Zhang, Induced multiple heterogeneities and related plastic improvement by laser surface treatment in CuZr-based bulk metallic glass, Intermetallics 24 (2012) 50-55.
[15] L. Hsu, J. Fang, D. Borca-Tasciuc, R. Worobo, C.I. Moraru, The effect of micro- and nanoscale topography on the adhesion of bacterial cells to solid surfaces, Appl. Environ. Microbiol. 79 (2013) 2703–2712.
[16] K.A. Whitehead, J. Colligon, J. Verran, Retention of microbial cells in substratum surface features of micrometer and sub-micrometer dimensions, Colloids Surf. B 41 (2005) 129–138
[17] R.S. Friedlander, H. Vlamakis, P. Kim, M. Khan, R. Kolter, J. Aizenberg, Bacterial flagella explore microscale hummocks and hollows to increase adhesion, Proc. Natl. Acad. Sci. 110 (2013) 5624–5629.
[18] Y. Zhu, J. Fu, C. Zheng, Z. Ji, Effect of nanosecond pulse laser ablation on the surface morphology of Zr-based metallic glass, Opt. Laser Tech. 83 (2016) 21-27.
[19] S. Marinier, L.J. Lewis, Femtosecond laser ablation of Cu x Zr 1− x bulk metallic glasses: a molecular dynamics study, Phys. Rev. B 92(18) (2015) 184108.
[20] I. Carvalho, M. Henriques, S. Carvalho, Microbial pathogens and strategies for combating them: science, technology and education Formatex research center2013.
[21] M.Á. Pacha-Olivenza, R. Tejero, M.C. Fernández-Calderón, E. Anitua, M. Troya, M.L. González-Martín, Relevance of topographic parameters on the adhesion and

proliferation of human gingival fibroblasts and oral bacterial strains, BioMed Res. Int. (2019).
[22] S. Shaikh, D. Singh, M. Subramanian, S. Kedia, A.K. Singh, K. Singh, N. Gupta, S. Sinha, Femtosecond laser induced surface modification for prevention of bacterial adhesion on 45S5 bioactive glass, J. Non-Cryst. Solids 482 (2018) 63-72.
[23] R.L. Taylor, J. Verran, G.C. Lees, A.P. Ward, The influence of substratum topography on bacterial adhesion to polymethyl methacrylate, J. Mater. Sci.: Mater. Med. 9 (1998) 17-22.
[24] K.J. Kubiak, M.C.T. Wilson, T.G. Mathia, P. Carval, Wettability versus roughness of engineering surfaces, Wear 271 (2011) 523-528.
[25] F. Song, H. Koo, D. Ren, Effects of material properties on bacterial adhesion and biofilm formation, J. Dent. Res. 94 (2015) 1027-1034.
[26] T. Wassmann, S. Kreis, M.Behr, R. Buergers, The influence of surface texture and wettability on initial bacterial adhesion on titanium and zirconium oxide dental implants, Int. J. Implant Dent. 3 (2017) 32.
[27] V.M. Villapún, S. Tardío, P. Cumpson, J.G. Burgess, L.G. Dover, S. González, Antimicrobial properties of Cu-based bulk metallic glass composites after surface modification, Surf. Coat. Tech. 372 (2019) 111-120.
[28] N.A. Burton, M.D. Johnson, P. Antczak, A. Robinson, P.A. Lund, Novel aspects of the acid response network of E. coli K-12 are revealed by a study of transcriptional dynamics, J. Mol. Biol. 401(5) (2010) 726-742.
[29] H. Huang, M. Jiang, J. Yan, Softening of Zr-based metallic glass induced by nanosecond pulsed laser irradiation, J. Alloys Compd. 754 (2018) 215-221.
[30] H. Huang, N. Jun, M. Jiang, M. Ryoko, J. Yan, Nanosecond pulsed laser irradiation induced hierarchical micro/nanostructures on Zr-based metallic glass substrate, Mater. Design 109 (2016) 153-161.
[31] N.M. Bulgakova, A.V. Bulgakov, Pulsed laser ablation of solids: transition from normal vaporization to phase explosion, Appl. Phys. A 73(2) (2001) 199-208.
[32] E. Williams, E.B. Brousseau, Nanosecond laser processing of Zr41.2Ti13.8Cu12.5Ni10Be22.5 with single pulses, J. Mater. Process. Tech. 232 (2016) 34-42.
[33] J. Fornell, E. Pellicer, E. Garcia-Lecina, D. Nieto, S. Suriñach, M.D. Baró, J. Sort, Structural and mechanical modifications induced on Cu47.5Zr47.5Al5 metallic glass by surface laser treatments, Appl. Surf. Sci. 290 (2014) 188-193.
[34] F.R. de Boer, R. Boom, W.C.M. Mattens, A.R. Miedema, A.K. Niessen, Cohesion in Metals: Transition Metal Alloys, North-Holland, Amsterdam, 1989.
[35] N. Li, T. Xia, L. Heng, L. Liu, Superhydrophobic Zr-based metallic glass surface with high adhesive force, Appl. Phys. Lett. 102(25) (2013) 251603.
[36] J. Ma, X.Y. Zhang, D.P. Wang, D.Q. Zhao, D.W. Ding, K. Liu, W.H. Wang, Superhydrophobic metallic glass surface with superior mechanical stability and corrosion resistance, Appl. Phys. Lett. 104(17) (2014) 173701.
[37] T. Xia, N. Li, Y. Wu, L. Liu, Patterned superhydrophobic surface based on Pd-based metallic glass, Appl. Phys. Lett. 101(8) (2012) 081601.
[38] K. Liu, L. Jiang, Metallic surfaces with special wettability, Nanoscale 3(3) (2011) 825-838.
[39] R.N. Wenzel, Resistance of solid surfaces to wetting by water, Ind. Eng. Chem. 28 (1936) 988-994.
[40] A.B.D. Cassie, S. Baxter, Wettability of porous surfaces, J. Chem. Soc. Faraday Trans. 40 (1944) 546-551.

[41] J.M. Romano, A. Garcia-Giron, P. Penchev, S. Dimov, Triangular laser-induced submicron textures for functionalising stainless steel surfaces, Appl. Surf. Sci. 440 (2018) 162-169.
[42] V.D. Ta, A. Dunn, T.J. Wasley, J. Li, R.W. Kay, J. Stringer, J.P. Smith, E. Esenturk, C. Connaughtond, J.D. Shephard, Laser textured surface gradients, Appl. Surf. Sci. 371 (2016) 583-589.
[43] D.V. Ta, A. Dunn, T.J. Wasley, R.W. Kay, J. Stringer, P.J. Smith, C. Connaughtond, J.D. Shephard, Nanosecond laser textured superhydrophobic metallic surfaces and their chemical sensing applications, Appl. Surf. Sci. 357 (2015) 248-254.
[44] F.M. Chang, S.L. Cheng, S.J. Hong, Y.J. Sheng, H.K. Tsao, Superhydrophilicity to superhydrophobicity transition of CuO nanowire films, Appl. Phys. Lett. 96(11) (2010) 114101.
[45] M. Rosenberg, H. Vija, A. Kahru, C.W. Keevil, A. Ivask, Rapid in situ assessment of Cu-ion mediated effects and antibacterial efficacy of copper surfaces, Sci. Rep. 8(1) (2018) 8172.
[46] V.M. Villapún, L.G. Dover, A. Cross, S. González, Antibacterial Metallic Touch Surfaces, Materials 9 (2016) 736.
[47] L.B. Boinovich, V.V. Kaminsky, A.G. Domantovsky, K.A. Emelyanenko, A.V. Aleshkin, E.R. Zulkarneev, I.A. Kiseleva, A.M. Emelyanenko, Bactericidal Activity of Superhydrophobic and Superhydrophilic Copper in Bacterial Dispersions, Langmuir 35(7) (2019) 2832-2841.
[48] L. Huang, E.M. Fozo, T. Zhang, P.K. Liaw, W. He, Antimicrobial behavior of cu-bearing zr-based bulk metallic glasses, Mater. Sci. Eng. C 39 (2014) 325-329.
[49] M. Hans, A. Erbe, S. Mathews, Y. Chen, M. Solioz, F. Mucklich, Role of Copper Oxides in Contact Killing of Bacteria, Langmuir 29 (2013) 16160–16166.

Laser texturing of BMGCs

T1: 0.70 J/cm²
T2: 1.39 J/cm²
T3: 2.82 J/cm²

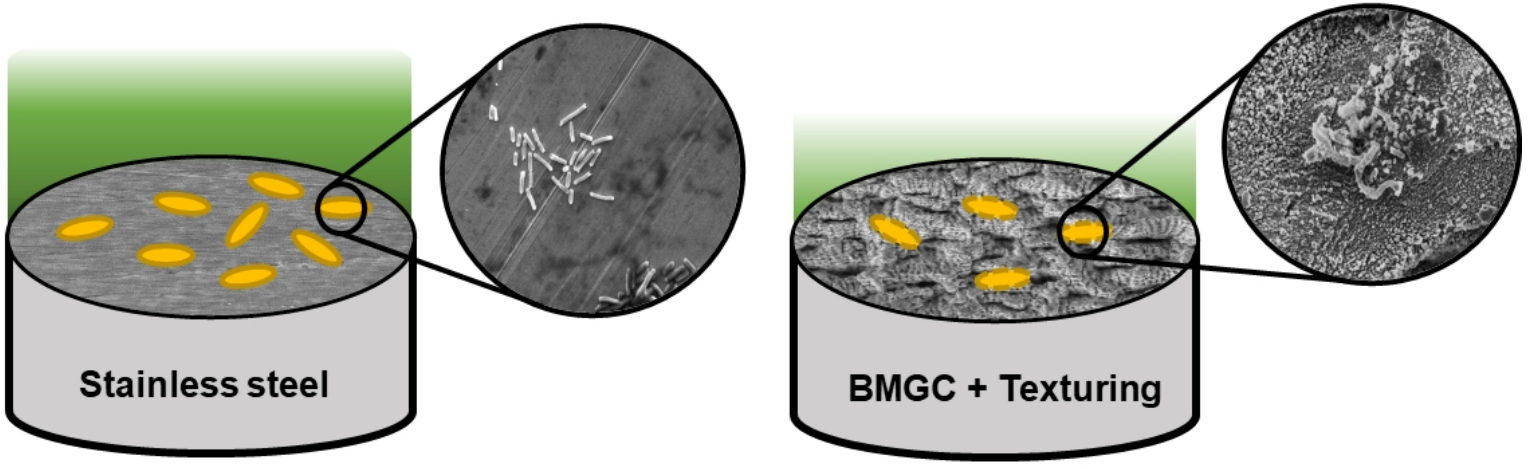

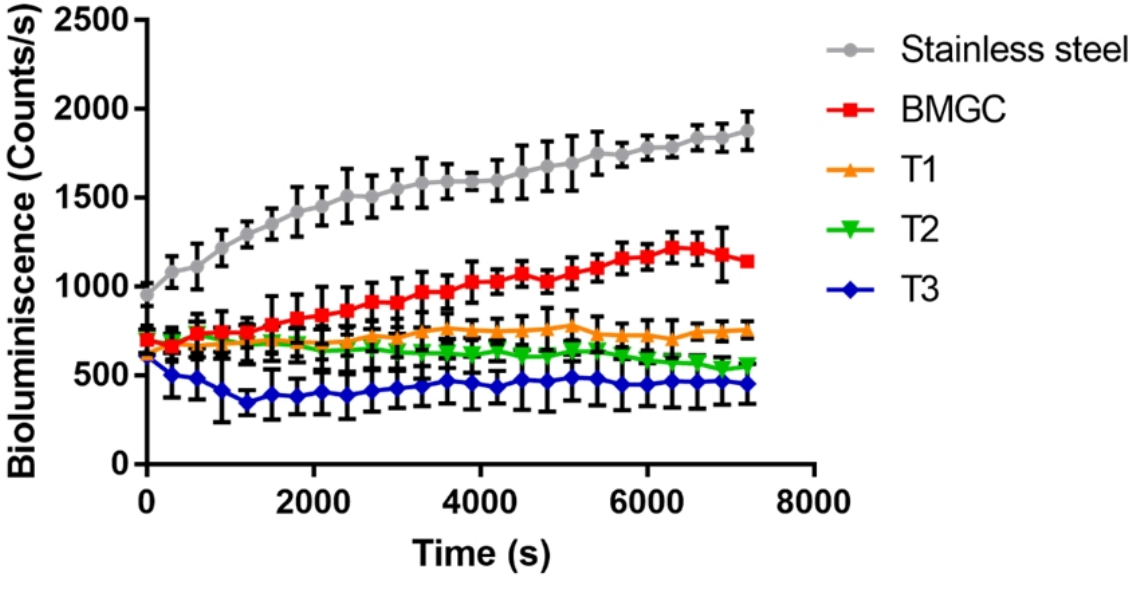

Stainless Steel

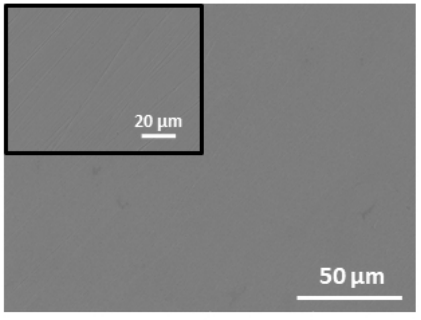

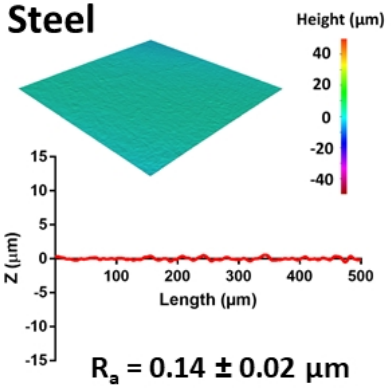

$R_a = 0.14 \pm 0.02$ µm

BMGC

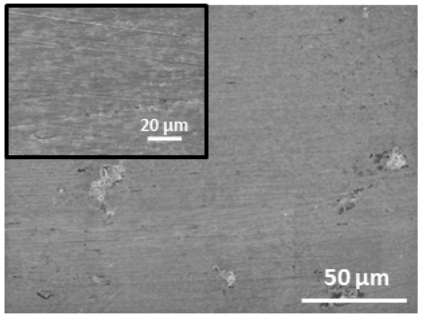

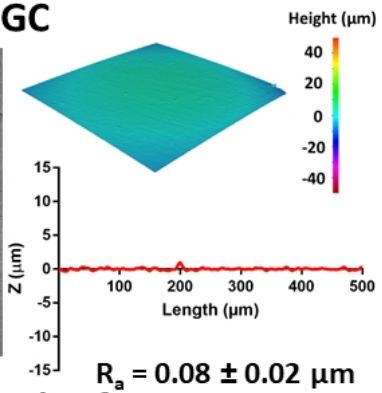

$R_a = 0.08 \pm 0.02$ µm

T1 (0.70 J/cm^2)

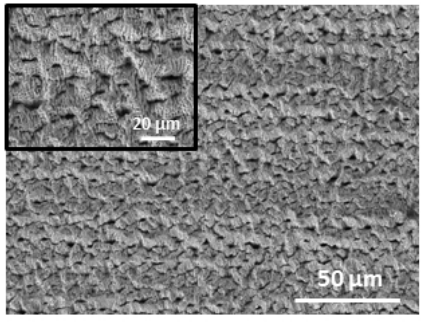

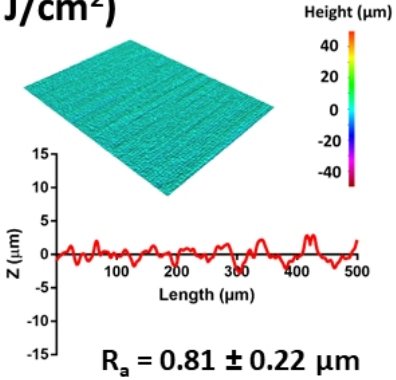

$R_a = 0.81 \pm 0.22$ µm

T2 (1.39 J/cm^2)

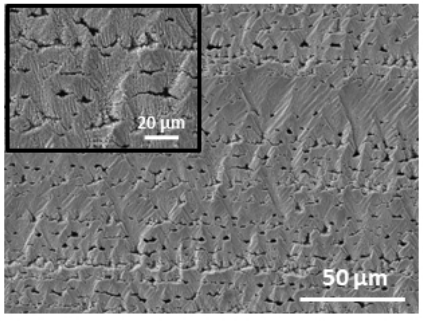

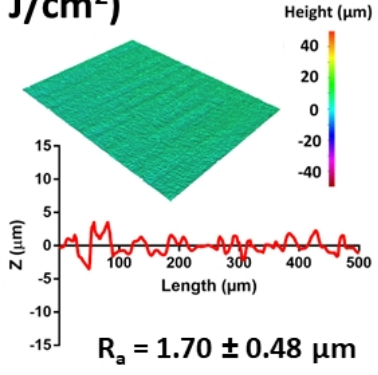

$R_a = 1.70 \pm 0.48$ µm

T3 (2.82 J/cm^2)

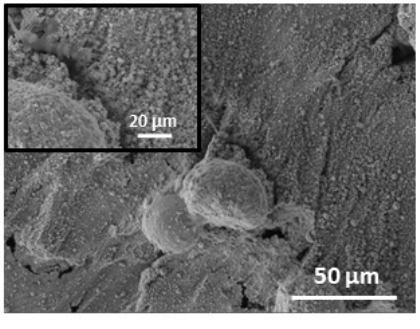

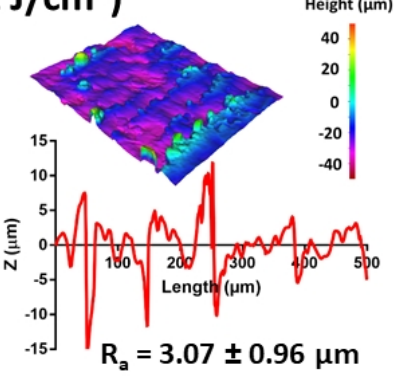

$R_a = 3.07 \pm 0.96$ µm

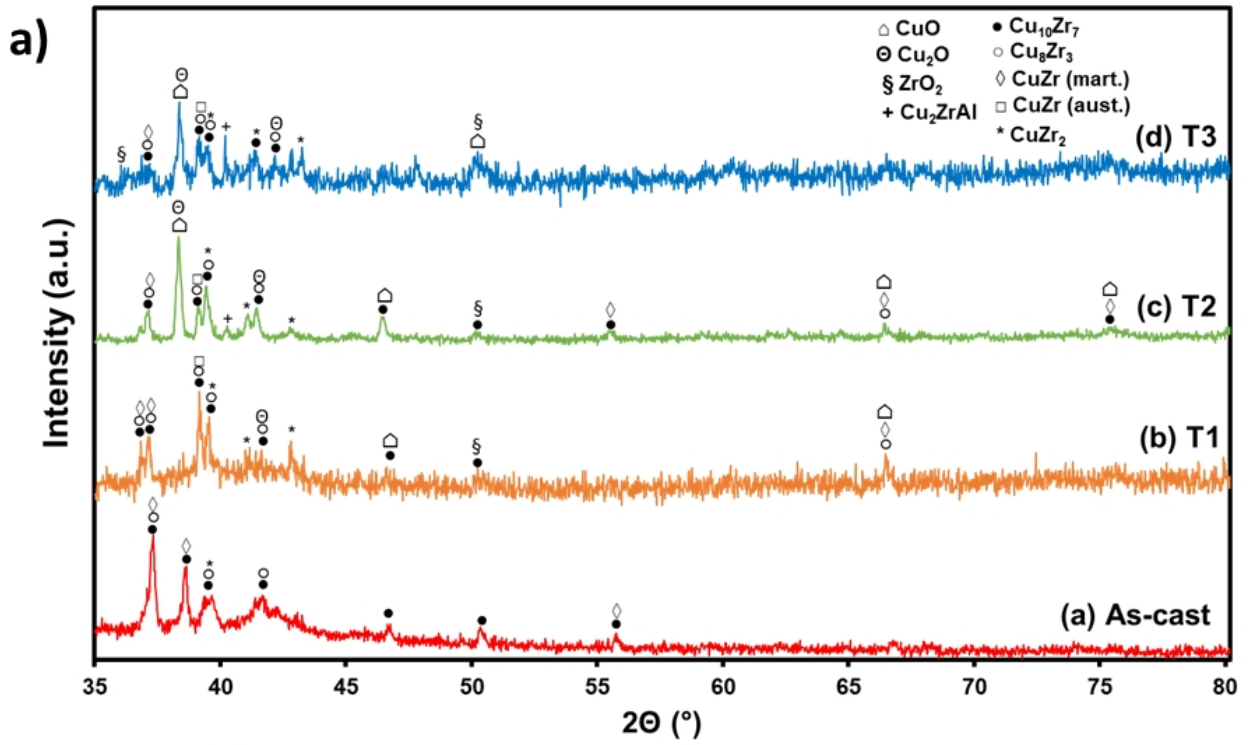
a)
CuO
Cu2O
ZrO2
Cu2ZrAl
Cu10Zr7
Cu8Zr3
CuZr (mart.)
CuZr (aust.)
CuZr2
(d) T3
(c) T2
(b) T1
(a) As-cast
Intensity (a.u.)
35
40
45
50
55
60
65
70
75
80
2Θ (°)

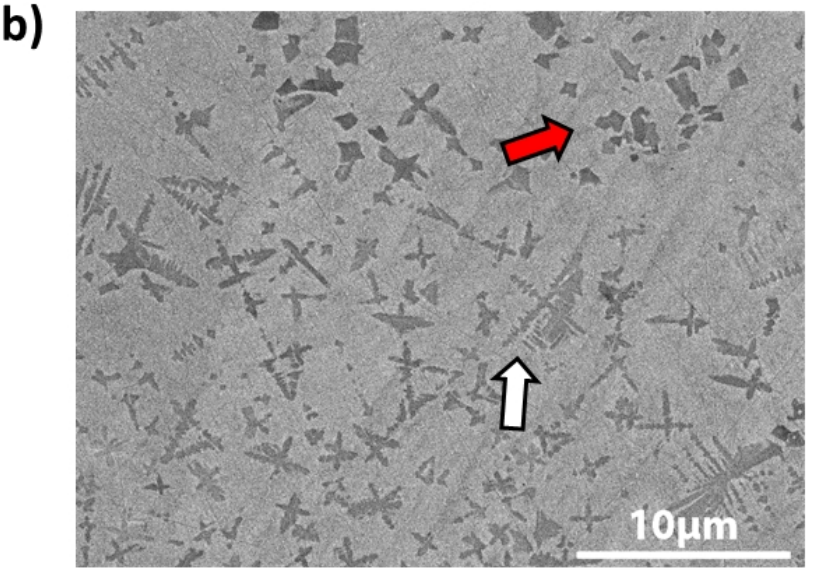
b)
10µm

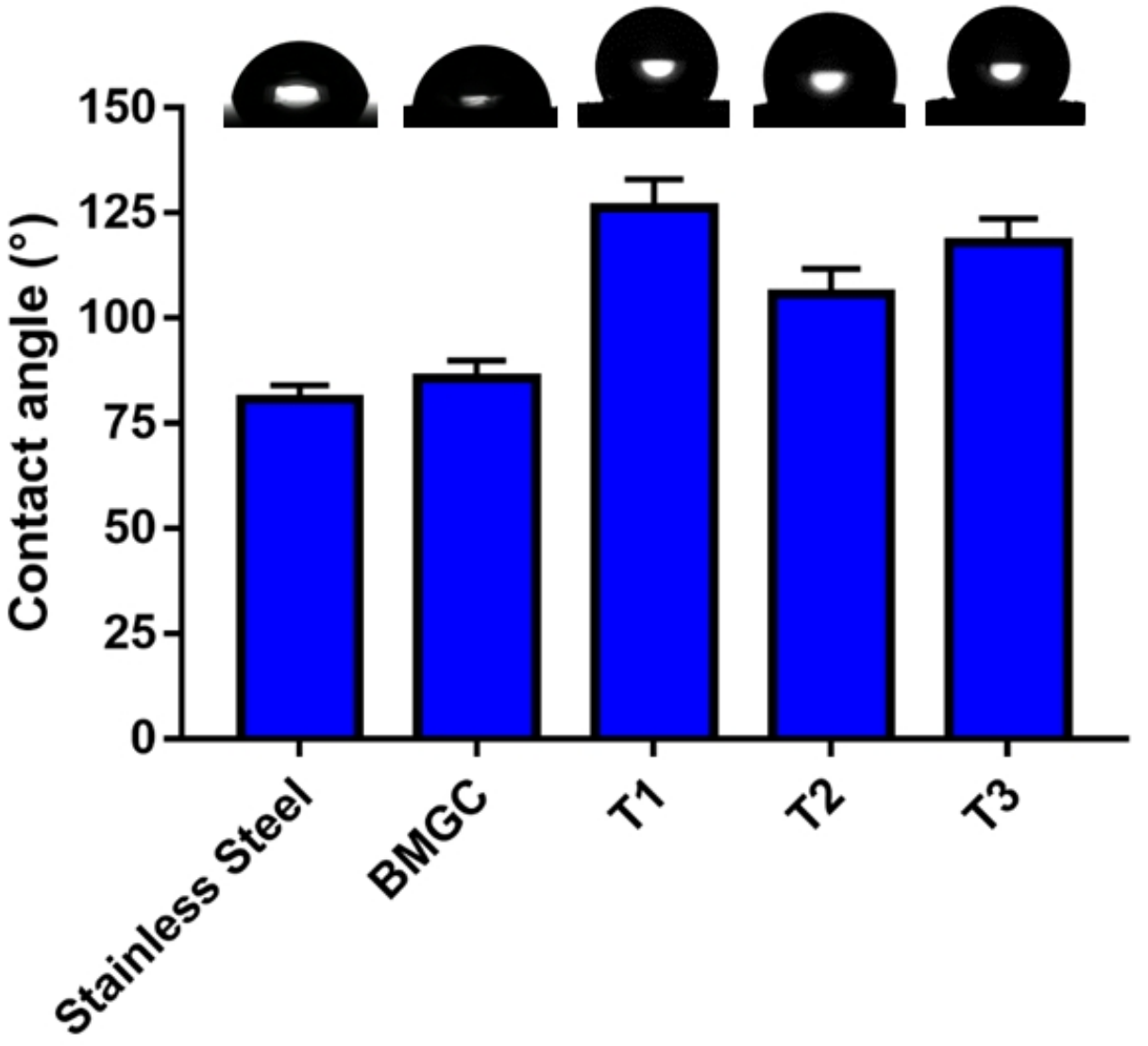
Contact angle (°)
150
125
100
75
50
25
0
Stainless Steel
BMGC
T1
T2
T3

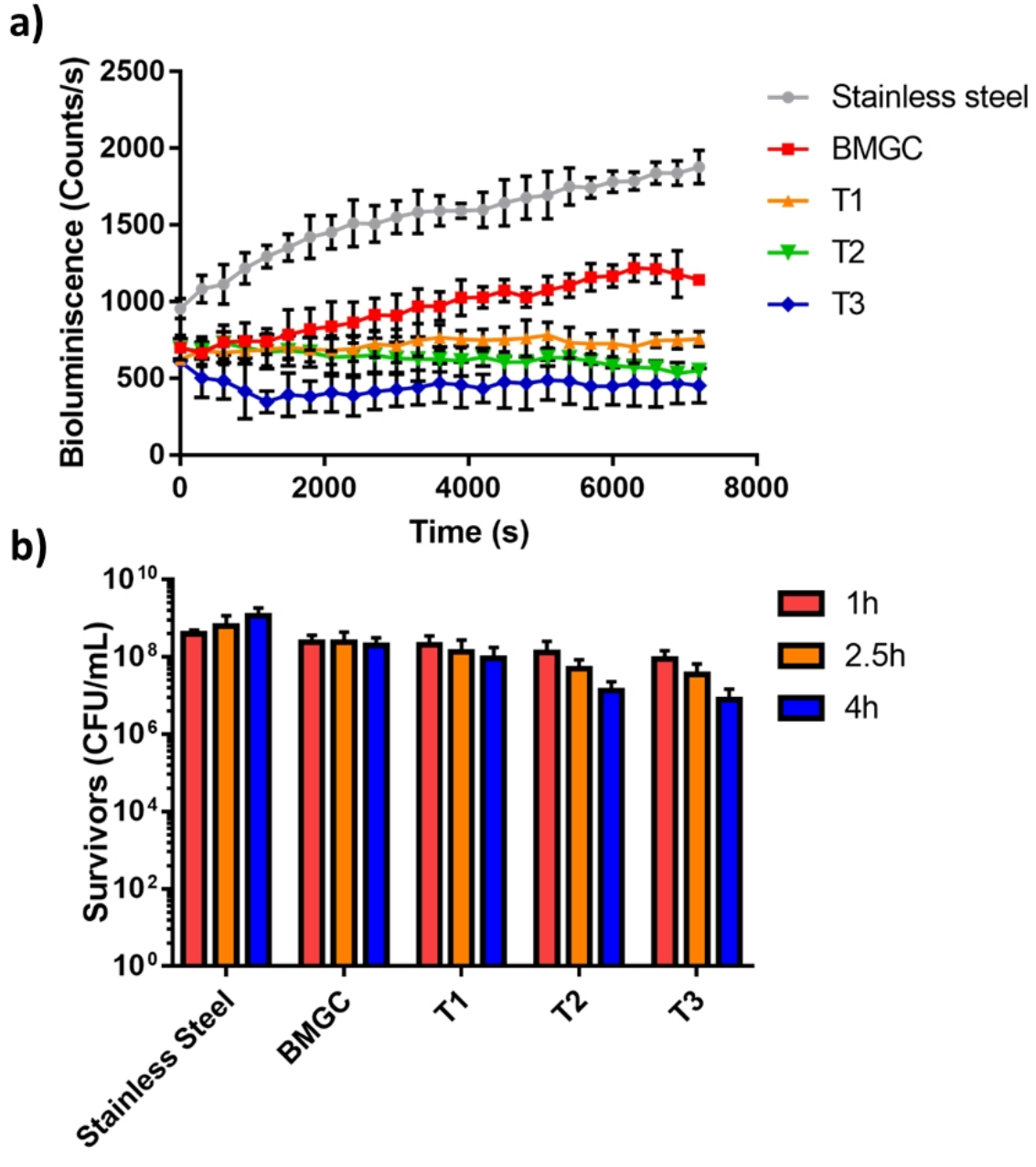
a)
Bioluminiscence (Counts/s)
2500
2000
1500
1000
500
0
0
2000
4000
6000
8000
Time (s)
Stainless steel
BMGC
T1
T2
T3
b)
Survivors (CFU/mL)
10^{10}
10^{8}
10^{6}
10^{4}
10^{2}
10^{0}
1h
2.5h
4h
Stainless Steel
BMGC
T1
T2
T3
c)
Stainless steel
4μm
BMGC
4μm
T1
4μm
T3
4μm

Conflict of Interest.

Declaration of interests

 The authors declare that they have no known competing financial interests or personal relationships that could have appeared to influence the work reported in this paper.

☐The authors declare the following financial interests/personal relationships which may be considered as potential competing interests: